# Imaging in Cartilage Restoration

3

Goetz H. Welsch

## Morphological MRI

To assess the state of the injured or painful joint, MRI is the method of choice. Besides bony structures (which can also be evaluated by radiographs), the soft tissue (ligament, menisci, fluid, and especially cartilage) within the joint can also be depicted. As recommended by the International Cartilage Repair Society (ICRS), standard morphological MR evaluation of cartilage repair tissue can be performed using the same acquisition techniques as those used for native cartilage or in OA [1]. Sufficient spatial resolution and signal-to-noise ratio (SNR) is essential for the diagnosis of cartilage alterations, as well as in the follow-up after cartilage repair procedures. Therefore, signal and resolution have to be high enough that the relatively thin cartilage layer can be visualized. While this is comparatively easy in the knee joint, it gets very demanding in joint like the hip or the ankle with clearly thinner cartilage layers. In addition to the cartilage, also the surrounding structures and all other structures in the joint need adequate characterization, as their condition factor into the individual therapy.

This leads to the following basic requirements for morphological MRI of cartilage:

1. The sequence protocol for the specific joint should be able to depict all important joint structures together with the cartilage layers.
2. For the visualization of articular cartilage, sufficient resolution (0.5 × 0.5 mm in-plane resolution) and sufficient SNR are needed.
3. The slice thickness should not exceed 3 mm. No larger interslice gap (20%) should be used.
4. The joint has to be assessed in all three planes, at least in one sequence.
5. The protocol has to include sequences with and without fat saturation or water excitation.
6. There should be one protocol for all cartilage patients to (i) detect cartilage defects or cartilage injuries, (ii) assess the cartilage repair tissue postoperatively (independently from the follow-up interval), and (iii) diagnose possible ongoing OA (unrelated to whether cartilage repair took place or not).
7. As mentioned above all joint structures (cartilage, menisci, ligaments, tendons, bone, fluid, synovial tissue) have to be assessed. In cartilage repair, besides the cartilage itself, the underlying (subchondral) bone has to be assessed in detail. Possible bony changes (edema, sclerosis, defects, etc.) have to be visualized.
8. The reproducibility of these measurements plays an important role especially when longitudinal evaluations are performed. Hence not only the sequence protocol has to be comparable, but also the localization of the joint and the planning of the sequence slabs have to be similar.

G. H. Welsch (✉)
UKE Athleticum, University Hospital Hamburg-Eppendorf (UKE), Hamburg, Germany



J. Farr, A. H. Gomoll (eds.), *Cartilage Restoration*, https://doi.org/10.1007/978-3-319-77152-6_3

9. If possible, the highest available field strength (3.0 Tesla) and a dedicated multi-channel joint coil have to be used.

Examples for basic knee MRI of cartilage and after cartilage repair can be found in Figs. 3.1, 3.2, and 3.3. Whereas Fig. 3.1 shows a volunteer without any cartilage pathology, Fig. 3.2 shows a patient with different pathologies of the knee joint (which would have a possible influence on cartilage therapy). Fig. 3.3 shows a patient after cartilage repair (microfracture therapy) by fat-saturated and non-fat-saturated proton-density turbo spin-echo (PD-TSE) MR sequences. This example shows, especially for the visualization of the subchondral bone, the importance of different contrasts for the evaluation of the cartilage repair tissue and the subchondral bone.

The specific sequences which have to be used for basic morphological MRI of cartilage are usually intermediate-weighted fast spin-echo (FSE)/turbo spin-echo (TSE) sequences or for cartilage evaluation fat-suppressed gradient-echo (GRE) acquisitions [1–5]. Whereas the GRE sequence visualizes cartilage defects attributable to T1 differences between cartilage and fluid, the FSE sequence uses differences in T2 weighting. Compared to fluid, cartilage is higher in signal intensity on fat-suppressed T1-weighting and lower on intermediate or T2-weighting. While the GRE sequence with fat suppression is suitable for visualization of the thickness and surface of

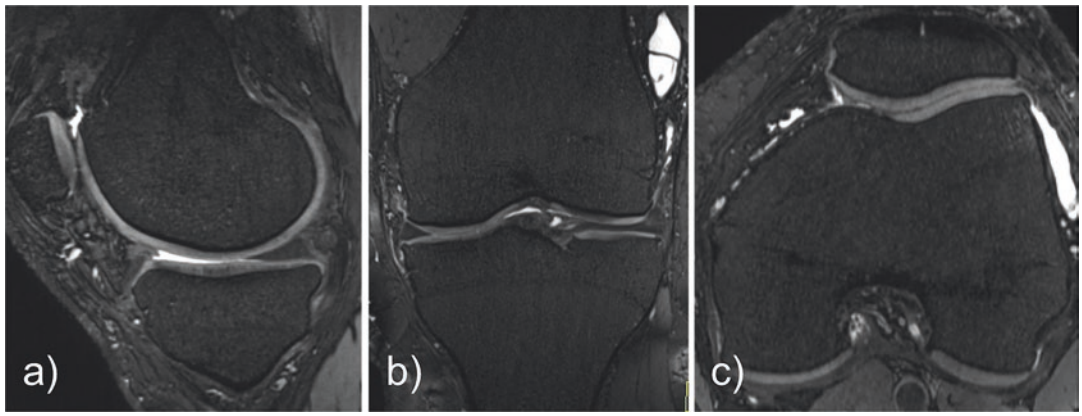


**Fig. 3.1** Morphological fat-saturated, proton-density turbo spin-echo (fsPD-TSE) MRI of a knee joint in three planes ((**a**): sagittal, (**b**): coronal, (**c**): axial). The images do not depict any cartilage pathology with homogeneous cartilage layers in all planes

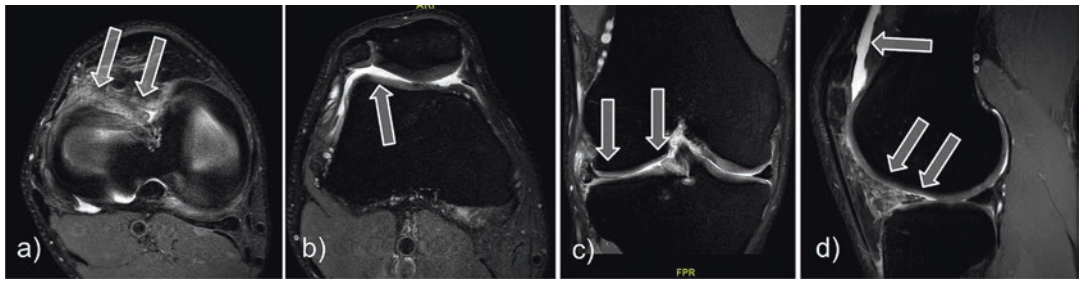


**Fig. 3.2** Morphological fat-saturated, proton-density turbo spin-echo (fsPD-TSE) MRI of a knee joint in three planes (**a**, **b**: axial, **c**: coronal, **d**: sagittal). Different pathological entities (marked by arrows) are present in this MRI that have possible consequences on the respective cartilage therapy. Meniscal degeneration with adjacent inflammation (**a**), bipartite patella (**b**), lateral cartilage thinning and extrusion of the lateral meniscus (**c**), meniscal degeneration with inflammation and increased joint fluid (**d**)

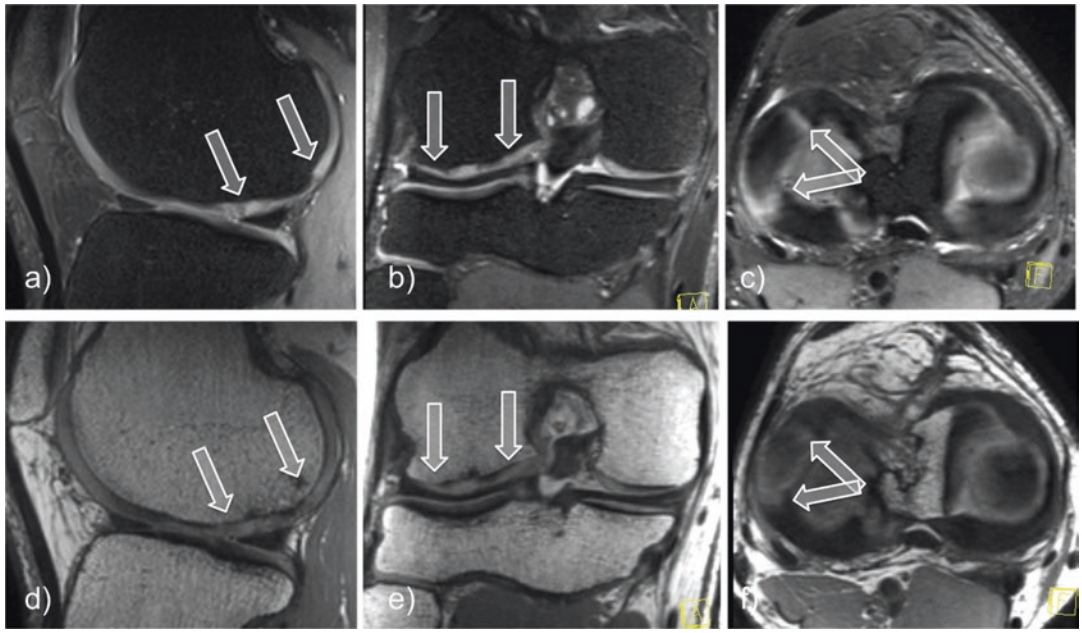


**Fig. 3.3** Morphological fat-saturated (**a**–**c**) and nonfat-saturated (**e**–**f**) PD-TSE MRI of a knee joint 36 months after microfracture therapy of the lateral femoral condyle (arrows) in three planes (**a**, **d**: sagittal, **b**, **e**: coronal, **c**, **f**: axial). Especially for the evaluation of the subchondral bone plate, the need for different contrast setting is observed. The images depict a clearly visible intralesional osteophyte (**a**) and subchondral sclerosis (**d**, **e**). The defect fill of the repair tissue is between 75% and 100%. The integration to the border zones is intact; the cartilage repair tissue shows slight signal alterations in comparison to the adjacent cartilage. No effusion in the joint is visible, no adhesions

cartilage and allows 3D volume measurements, the FSE sequence is sensitive for the assessment of the internal cartilage structure as well [1, 2, 4]. The subchondral bone also displays high signal intensity, due to fatty marrow, which remains relatively hyperintense on FSE T2 sequences. Intrachondral cartilage matrix alterations, surface changes, and fibrillation can thus be assessed. Another advantage of FSE sequences is the low sensitivity to magnetic susceptibility artifacts, which facilitates the reliable use postoperatively. Both sequences, the fat-suppressed 3D GRE and the T2-weighted FSE, have shown excellent results, with high sensitivity, specificity, and accuracy for detecting cartilage lesions in the knee [1, 2, 6]. These sequences can also be used for morphological assessment after cartilage repair using the magnetic resonance observation of cartilage repair tissue (MOCART) scoring system [7, 8].

## Cartilage Injuries and Cartilage Lesions

As mentioned above, the evaluation of acute/traumatic cartilage injuries, chronic cartilage lesions, or even ongoing osteoarthritic changes is based on the same set of sequences. Therefore, the respective MR protocol has to provide the cartilage layers with high enough resolution and signal (SNR). The depiction of the grade of a cartilage defect is based on different grading systems. One of the most common and practical scores is the ICRS grading system. The different grades within this system can be assessed by MRI and are helping to provide the respective diagnosis for the surgeon and may be part of the preoperative decision making. The true size and grade, however, shows in many studies great variance between the preoperative MRI and the surgical procedure, especially since the precise

borders of the cartilage defect cannot be sufficiently detected by MRI. Furthermore, very early cartilage alterations, as described by ICRS grade 1 for superficial cartilage lesions, superficial fissures, and cracks, can only be assessed by high-resolution MRI as shown in Fig. 3.4. This image, however, is based on a 7 Tesla MRI, where high enough signal is available, and in-resolutions of up to 0.2 × 0.2 mm are possible. Higher grades of cartilage defects can be detected more easily by means of MRI, and the needed resolution can be decreased (~0.4 × 0.4 mm). These lesions are described as ICRS grade 2 with lesions extending to <50% of cartilage depth and ICRS grade 3 with cartilage defects extending down to >50% of cartilage depth. Examples are provided in Fig. 3.5. Figures 3.4 and 3.5 illustrate the challenge of correctly assessing the grade of cartilage defect by means of MRI, with a strong observer dependency, important since one main aim of MRI is to help decide which cartilage lesions need surgical intervention and others that do not. ICRS grade 4 lesions are complete cartilage lesions, where the subchondral bone is exposed and no cartilage is left (Fig. 3.6). These lesions, compared to all other lesions, may be acute or chronic cartilage lesions. A recent approach to grade cartilage lesions more easily, with a possible better usefulness for the orthopedic surgeon and preoperative

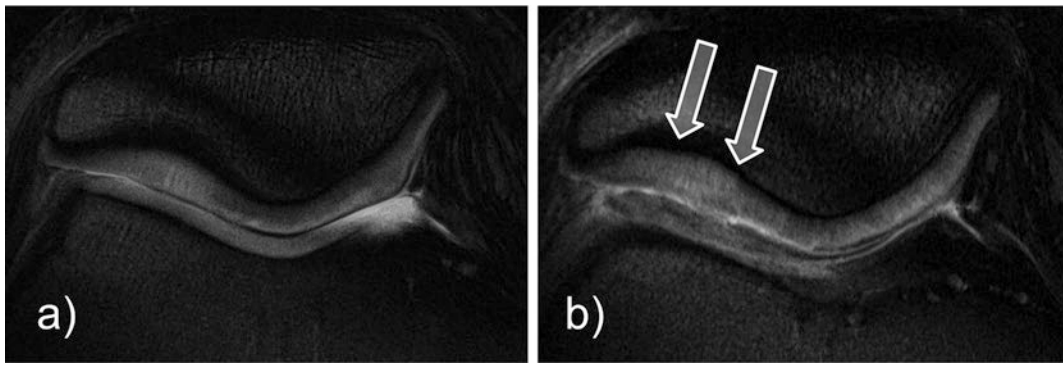


**Fig. 3.4** Very-high-resolution morphological fsPD-TSE axial MR images of the patellofemoral joint as performed on a 7.0 Tesla MRI with an in-plane resolution of 0.2 × 0.2 mm. The left image (**a**) shows normal healthy cartilage structure (ICRS grade 0), whereas the right image (**b**) shows superficial cartilage fibrillation (arrows) (ICRS grade 1)

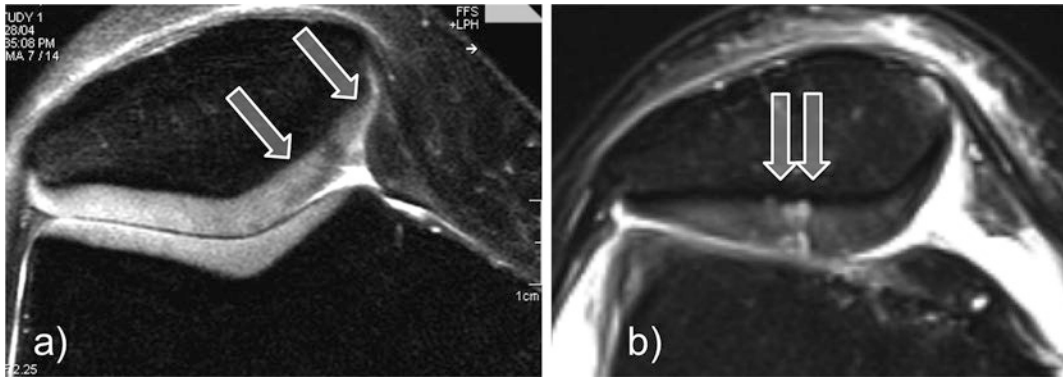


**Fig. 3.5** High-resolution morphological fsPD-TSE axial MR images of the patellofemoral joint as performed on a 3.0 Tesla MRI with an in-plane resolution of 0.4 × 0.4 mm. The left image (**a**) shows abnormal cartilage with lesions extending down to <50% of cartilage depth (ICRS grade 2), whereas the right image (**b**) shows severely abnormal cartilage with defects extending down >50% of cartilage depth (ICRS grade 3)

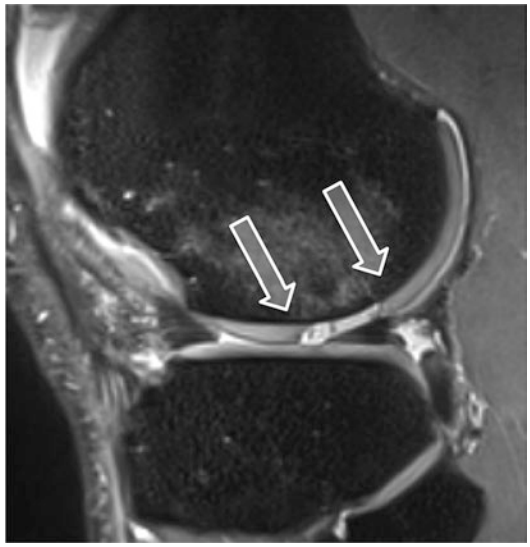

**Fig. 3.6** High-resolution morphological fsPD-TSE sagittal MR images of the femorotibial joint as performed on a 3.0 Tesla MRI with an in-plane resolution of 0.4 × 0.4 mm. The image shows a complete traumatic cartilage defect (ICRS grade 4), with underlying bone marrow edema

decision making, is the so-called AMADEUS (Area Measurement And DEpth and Underlying Structures) score. This is a preoperative scoring and classification system for the assessment of preoperative cartilage defect severity including the parameters [1] cartilage defect size, [2] depth/morphology of the cartilage defect, and [3] subchondral bone quality, resulting in a specific three-digit code and a numeric score of 0–100 points [9].

While the widely applied MOCART score is used for postoperative assessment after cartilage repair surgery, the new AMADEUS score was designed to provide an easy and intuitive measure for chondral defects prior to a possible surgical intervention.

This score has one very important goal, which is to improve communication between the diagnosis of the radiologist and the decision making of the orthopedic surgeon. Even more, it may deliver a semiquantitative score to provide a predictor for the success of cartilage restoration, especially when using the MOCART score postoperatively. The AMADEUS score is provided in Table 3.1.

**Table 3.1** AMADEUS (Area Measurement and Depth and Underlying Structures) score

| AMADEUS feature | Points |
|---|---|
| **1. Area measurement** | |
| Defect size in $cm^2$ (largest diameter sagittal x coronal) | |
| ○ No defect | (40) |
| ○ ≤1 $cm^2$ | (35) |
| ○ >1 to ≤2 $cm^2$ | (30) |
| ○ >2 to ≤4 $cm^2$ | (20) |
| ○ >4 to ≤6 $cm^2$ | (10) |
| ○ >6 $cm^2$ | (0) |
| **2. Defect depth** | |
| (n) No defect | (20) |
| (a) Signal alteration | (15) |
| (b) Partial-thickness defect | (10) |
| (c) Full-thickness defect | (0) |
| **3. Underlying structures** | |
| Subchondral bone defect | |
| A. No defect | (30) |
| B. Bony defect/ cyst ≤5 mm depth | (20) |
| C. Bony defect/ cyst >5 mm depth | (0) |
| **4. Addendum – potential forth digit** | |
| D. No defect-associated bone marrow edema | (10) |
| E. Defect-associated bone marrow edema | (0) |
| **AMADEUS total score** | **(100)** |
| **AMADEUS grade** | **(0 worst, 100 best)** |
| **Grade I** | **>75** |
| **Grade II** | **>50 and ≤75** |
| **Grade III** | **>25 and ≤50** |
| **Grade IV** | **≤25** |

This leads to the following basics for morphological MRI of cartilage lesions:

1. ICRS grading system as valid method to assess cartilage defects using MRI as well as surgery.
2. The AMADEUS score is a new preoperative scoring and classification system.
3. The sensitivity and specificity of MRI in terms of depicting the different grades of cartilage lesions is low for early cartilage lesions and improves with higher grades of cartilage defects.
4. For MRI, resolution and signal are playing an important role to assess the respective cartilage lesion in the highest possible quality and thus reliability.

5. Although MRI cannot depict the cartilage lesion with very high sensitivity or specificity, MRI is one of the most important tools for surgical decision making.

While the accuracy of the structural diagnosis is an integral part when treating patients, the age of the patient, the activity level, the symptoms, and other clinical findings are also of utmost importance when planning surgery. Hence, besides the clinical evaluation, the preoperative MRI also needs to be of high quality, especially as existing studies show that radiologic reports based on standard morphological MRI frequently underestimate the actual size of a lesion (which were then found intraoperatively) [10, 11]. In the study by Gomoll and coworkers, cartilage lesions were underestimated up to 300% in the patellofemoral joint [11]. Based on a high-quality MRI, this should not be the case, and cartilage lesions should be graded more accurately. As shown in Figs. 3.4, 3.5, and 3.6, high resolution and signal help to define the grade of cartilage damage as well as the size of the cartilage defect.

Nonetheless it will never be possible to obtain perfect correlation between noninvasive diagnostics and direct observation during surgery; on the other hand, to plan a tailored surgical approach, correlation needs to improve. The preoperative underestimation of cartilage lesion size is based on different reasons. First, a standard MRI usually consists of 2D sequences with a slice thickness of approximately 3 mm and an existing interslice gap. Hence the borders of the cartilage defect are not exactly depicted. Furthermore there are regions in the knee (e.g., the trochlea) where the assessment of the anatomy is not possible by 2D MR sequences. Possibly, better results can be reached by utilizing isotropic MR sequences [12, 13]. With these sequences, a 3D data set can be acquired (e.g., $0.5 \times 0.5 \times 0.5$ mm) without any gap between the slices. Using 3D viewing tools, the observer can navigate three-dimensionally within the knee joint, and all anatomical regions can be graded adequately. Besides morphological MRI, also biochemical MR sequences, such as dGEMRIC (delayed Gadolinium-Enhanced MRI of Cartilage), T2 mapping, T1rho, CEST (chemical exchange saturation transfer), or others, can be used in preoperative imaging. Although a full-thickness cartilage defect cannot be evaluated, biochemical MRI is a very promising tool to (i) assess the borders of the cartilage defect regarding their quality, to (ii) assess the cartilage defect itself if there is not a full-thickness defect, and (iii) to assess the cartilage quality of the surrounding tissue. Although only limited studies are available on the preoperative utilization of biochemical MR techniques, the provided examples might be topics of future research and could help in clinical decision making. By including biochemical MRI, initial studies showed that early cartilage changes can be detected and quantified [14, 15].

In conclusion, preoperative MRI (respectively optimal cartilage diagnosis) should contain a set of cartilage-sensitive MR sequences and, whenever possible, a 3D isotropic MR sequence, as well as (if possible) a biochemical MR sequence. Moreover the remainder of the joint has to be assessed in sufficient detail.

## Cartilage Repair Tissue

The depiction of cartilage repair tissue after cartilage restoration using MRI is a very important part of current clinical routine. Good clinical and radiological outcome are the goal to potentially postpone the development of OA in the treated joint. Besides clinical routine, research investigations are using MRI as a measure of successful treatment [16, 17]. After surgical intervention, the cartilage repair tissue and the surrounding structures can be assessed semiquantitatively by the MOCART score [13]. Furthermore, including the whole joint, the recently introduced CROAKS score is able to assess the repair tissue as well as the rest of the joint [18]. As cartilage repair mainly tries to postpone the onset or the development of OA, it is very important to include the rest of the joint into existing imaging strategies.

The basis for evaluation of the repair tissue nevertheless is the MOCART score which has to be assessed by a consistent cartilage-sensi-

tive imaging protocol. Hence an optimal MRI protocol after a cartilage repair procedure should in principle contain the same set of sequences as the preoperative MRI. One exception is due to the fact that the area where the repair procedure was performed is now known. This area can be depicted in more detail in the highest possible resolution. The planning of such a sequence slab is based on the anatomical area (e.g., the medial femoral condyle) where cartilage repair took place. By exploiting high resolution in this limited area of cartilage repair, early changes like beginning delimitation, subtle split-like lesions, or underlying bony changes can be diagnosed and possibly treated with the aim to prevent the patient from a failure of the repair procedure.

As mentioned above, in the postoperative follow-up, the magnetic resonance observation of cartilage repair tissue (MOCART) scoring system is utilized to allow subtle and suitable assessment of the articular cartilage repair tissue [7, 8]. This MR assessment of the MOCART score is based on standard 2D MR sequences, depending on the locality of the area of cartilage repair. The MR evaluation of the cartilage repair tissue is performed on sagittal, axial, or coronal planes using high spatial resolution together with a slice thickness up to 3 mm. However, this MOCART scoring system can now be performed in more detail and with additive variables, enabling for a more precise depiction of the repair tissue as well as the surrounding structures. This new "3D" MOCART score [13] can still be assessed by 2D standard MR sequences; however, the new and abovementioned 3D isotropic MR sequences can also be used, and their potential benefits are incorporated into this new score. In literature, this score seems to be reproducible and can be achieved by different MR protocols and in different joints besides the knee joint [12, 13]. A scoring sheet for the new MOCART score is presented

**Table 3.2** Three-dimensional (3D) magnetic resonance observation of cartilage repair tissue (MOCART) score using an isotropic 3D MR sequence

| **Variables** |
|---|
| **1. Defect fill** (degree of defect repair and filling of the defect in relation to the adjacent cartilage) |
| ○ 0% |
| ○ 0–25% |
| ○ 25–50% |
| ○ 50–75% |
| ○ 75–100% |
| ○ 100% |
| ○ 100–125% |
| ○ 125–150% |
| ○ 150–200% |
| ○ >200% |
| Localization |
| ○ Whole area of cartilage repair ○ >50% ○ <50% |
| ○ Central ○ Peripheral ○ Weight-bearing ○ Non-weight-bearing |
| **2. Cartilage interface** (integration with adjacent cartilage to border zone in two planes) |
| Sagittal (femur, patella, trochlea, tibia) |
| ○ Complete |
| ○ Demarcating border visible (split-like) |
| ○ Defect visible <50% |
| ○ Defect visible >50% |
| Coronal (femur, tibia); axial (patella, trochlea) |
| ○ Complete |
| ○ Demarcating border visible (split-like) |

(continued)

**Table 3.2** (continued)

| |
|---|
| ○ Defect visible <50% |
| ○ Defect visible >50% |
| Localization |
| ○ Whole area of cartilage repair ○ >50% ○ <50% |
| ○ Weight-bearing ○ Non-weight-bearing |
| **3. Bone interface** (integration of the transplant to the subchondral bone; integration of a possible periosteal flap) |
| ○ Complete |
| ○ Partial delamination |
| ○ Complete delamination |
| ○ Delamination of periosteal flap |
| Localization |
| ○ Weight-bearing ○ Non-weight-bearing |
| **4. Surface** (constitution of the surface of the repair tissue) |
| ○ Surface intact |
| ○ Surface damaged <50% of depth |
| ○ Surface damaged >50% of depth |
| ○ Adhesions |
| Localization |
| ○ Whole area of cartilage repair ○ >50% ○ <50% |
| ○ Central ○ Peripheral ○Weight-bearing ○ Non-weight-bearing |
| **5. Structure** (constitution of the repair tissue) |
| ○ Homogeneous |
| ○ Inhomogeneous or cleft formation |
| Localization |
| ○ Whole area of cartilage repair ○ >50% ○ <50% |
| ○ Central ○ Peripheral ○ Weight-bearing ○ Non-weight-bearing |
| **6. Signal intensity** (intensity of MR signal in of the repair tissue in comparison to the adjacent cartilage) |
| ○ Normal (identical to adjacent cartilage) |
| ○ Nearly normal (slight areas of signal alteration) |
| ○ Abnormal (large areas of signal alteration) |
| Localization |
| ○ Central ○ Peripheral ○ Weight-bearing ○ Non-weight-bearing |
| **7. Subchondral lamina** (constitution of the subchondral lamina) |
| ○ Intact |
| ○ Not intact |
| Localization |
| ○ Whole area of cartilage repair ○ >50% ○ <50% |
| ○ Central ○ Peripheral ○ Weight-bearing ○ Non-weight-bearing |
| **8. Chondral osteophytes** (osteophytes within the cartilage repair area) |
| ○ Absent |
| ○ Osteophytes <50% of the thickness of the cartilage transplant |
| ○ Osteophytes >50% of the thickness of the cartilage transplant |
| Localization |
| Size: _____ mm (plane: _____) x _____ mm (plane: _____) |
| ○ Central ○ Peripheral ○ Weight-bearing ○ Non-weight-bearing |
| **9. Bone marrow edema** (maximum size and localization in relation to the cartilage repair tissue and other alterations assessed in the 3D MOCART score) |
| ○ Absent |
| ○ Small (<1 cm) |
| ○ Medium (<2 cm) |

(continued)

**Table 3.2** (continued)

| |
|---|
| ○ Large (<4 cm) |
| ○ Diffuse |
| Localization |
| Size: _____ mm (plane: _____) x _____ mm (plane: _____) |
| ○ Central ○ Peripheral ○ Weight-bearing ○ Non-weight-bearing |
| ○ Relation to other alterations within this score of variable No. _____ |
| **10. Subchondral bone** (constitution of the subchondral bone) |
| ○ Intact |
| ○ Granulation tissue |
| ○ Cyst |
| ○ Sclerosis |
| Localization |
| ○ Whole area of cartilage repair ○ >50% ○ <50% |
| ○ Central ○ Peripheral ○ Weight-bearing ○ Non-weight-bearing |
| **11. Effusion** (approx. size of joint effusion visualized in all planes) |
| ○ Absent |
| ○ Small |
| ○ Medium |
| ○ Large |

Variables 1–11 for 3D MOCART score; subcategories "localization" optional

in Table 3.2. Examples of MR images after cartilage repair can be seen in Fig. 3.3. Figure 3.7 illustrates the possibilities of a 3D isotropic data set where the cartilage repair tissue can be assessed in every plane and especially the border zones and the integration of the repair tissue can be accurately assessed.

This leads to the following basics for morphological MRI after cartilage repair:

1. There should be one consistent protocol for all patients to (i) detect cartilage defects or cartilage injuries, (ii) assess the cartilage repair tissue postoperatively (independently from the follow-up interval), and (iii) diagnose possible degenerative changes (unrelated to whether cartilage repair took place or not).
2. Based on the area of cartilage repair, an additional, high-resolution sequence can be obtained only of the area of cartilage repair to depict the repair tissue in greater detail.
3. Based on the new MOCART score with its 11 variables, the repair tissue as well as all the surrounding tissues can be assessed. This score can either be used to (i) semiquantitatively score the effects of the surgical procedure longitudinally, (ii) compare different patients or different repair procedures with each other (e.g., in clinical studies), or (iii) serve the radiologist or the orthopedic surgeon as a tool to diagnose the area of cartilage repair step by step in a validated way.
4. Isotropic MR sequences can serve to assess the area of cartilage repair in even greater detail and to visualize the borders of the repair tissue also in anatomically challenging areas.

Additionally, the whole joint has to be taken into consideration when assessing a knee joint after cartilage repair. Although the clinical indications for cartilage repair surgery include, in addition to persistent pain and limitation in function, a defined cartilage defect and ideally no associated features of osteoarthritis, this is not always the case. Furthermore, OA can develop over time in any patient. While the value of the MOCART score is to evaluate the repair site, including different parameters (Table 3.2) such as filling of the defect, integration to the repair site borders, or subchondral bone changes, the remaining joint has been largely ignored in MR studies on the success of cartilage repair. Hence,

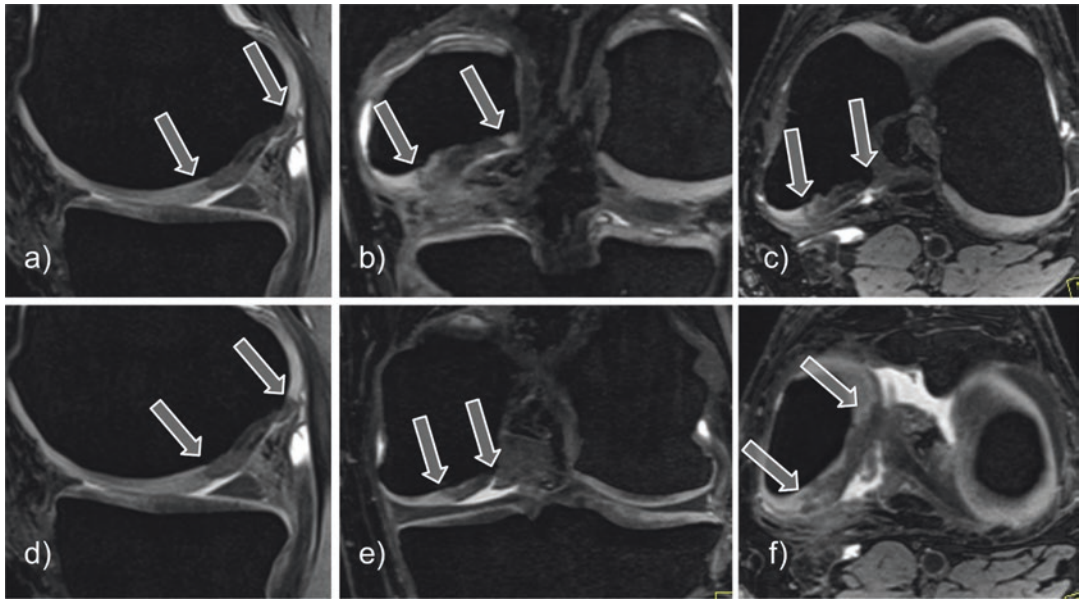


**Fig. 3.7** High-resolution morphological isotropic (0.5 × 0.5 × 0.5 mm) fat-saturated 3D PD-SPACE [sampling perfection with application-optimized contrasts using different flip angle evolutions] sequence of a patient 24 months after matrix-associated autologous chondrocyte transplantation (MACT) of the medial femoral condyle. The data set provides different multi-planar reconstructions (MPRs) of the area of cartilage repair (arrows). The defect fill is 100%; the cartilage repair tissue is well integrated in every given plane (**a**, **d**: sagittal; **b**, **e**: coronal; **c**, **f**: axial). There is no bone marrow edema visible; other bony irregularities, however, cannot be assessed on the fat-saturated sequence. The structure of the repair tissue is inhomogeneous and hypo-intense showing slight signal alteration. No effusion or adhesion is visible

only the repair tissue itself and the directly surrounding cartilage have been analyzed [16, 19]. Nevertheless, the ultimate goal of preventing osteoarthritis can only be proven if the whole joint is assessed including the different tissues that are integral to the joint disease. Different whole-joint MRI scoring systems for MRI assessment of osteoarthritis such as the Whole-Organ Magnetic Resonance Imaging Score (WORMS), Knee Osteoarthritis Scoring System (KOSS), Boston-Leeds Osteoarthritis Knee Score (BLOKS), and MRI Osteoarthritis Knee Score (MOAKS) have been introduced, and their reliability and validity have been proven in multiple studies [20–22]. However, theses scores are not applicable for cartilage repair, since they do not take the area where repair has taken place into account. Very recently the so-called cartilage repair osteoarthritis knee score (CROAKS) has been introduced with a detailed description of the assessment of the whole joint together with the area of cartilage repair [18]. This score combined the MOCART score together with the MOAKS score and will provide a very valid tool in thoroughly assessing the success of cartilage repair, especially on its ultimate goal, which is to prevent or postpone OA. The introduction of the CROAKS demonstrated the score to be feasible and reliable [18]; further upcoming studies will have to prove its scientific and clinical merit.

## Biochemical MRI

Studies on the preoperative assessment of cartilage (before cartilage restoration is performed) using biochemical (compositional) MRI are relatively rare. Nevertheless a recent study validating T2 mapping by arthroscopy showed that in partial- or full-thickness cartilage lesions (ICRS grade 3 and 4), but also in lower-graded cartilage lesions (ICRS grade 1

and 2), there is a high correlation between intraoperative findings and quantitative T2 mapping [23], especially in the postoperative follow-up after cartilage repair. However, biochemical MR sequences provide additional information on the ultrastructure and the composition of the cartilage repair tissue and the surrounding cartilage. T1 mapping using the dGEMRIC technique, T2 mapping, T1 rho, diffusion-weighted imaging, and many other techniques show very promising results in different research studies and even in early clinical applications [24–28]. Different types of repair tissues (e.g., MACT versus MFX) can be clearly distinguished, and the quality of the repair tissue can be assessed noninvasively. Furthermore, different matrices used for MACT can be imaged and quantified in their ability to produce hyaline-like repair tissue. Additionally the maturation of the cartilage repair tissue over time can be analyzed, and the reorganization of the collagen matrix or the expansion of proteoglycans can be demonstrated. While there are techniques that can visualize the proteoglycan or glycosaminoglycan (GAG) content, there are other techniques which are more specific for the collagen matrix.

## Glycosaminoglycan (GAG)-Sensitive Techniques

The most frequently used technique for the quantification of the GAG content is T1-dGEMRIC (delayed gadolinium-enhanced MRI of cartilage). Intravenously administered gadolinium diethylenetriamine pentaacetate anion ($Gd\text{-}DTPA^{2-}$) penetrates the cartilage through the subchondral bone and especially through the synovial fluid. The contrast equilibrates in inverse relation to the fixed charge density (FCD), which is, in turn, directly related to the GAG concentration; therefore, T1, which is determined by the $Gd\text{-}DTPA^{2-}$ concentration, becomes a specific measure of tissue GAG concentration, suggesting that $Gd\text{-}DTPA^{2}$-enhanced MRI has the potential for monitoring GAG content of cartilage in vivo [29]**.** Thus, T1 mapping enhanced by $Gd\text{-}DTPA^{2-}$ (T1 dGEMRIC) was for many years the method of choice for quantifying proteoglycan depletion in articular cartilage [30, 31].

There are existing studies which propose that the pre-contrast T1 values must be calculated, in addition to the real "delayed"-enhanced post-contrast T1 values [32]. More recent studies that improve the clinical relevance of this technique show nevertheless the ability to only use the post-contrast T1-dGEMRIC mapping values without any loss of information on the constitution of the cartilage repair tissue [33]. Concerning the cartilage repair tissue quality, a study showed dGEMRIC to be able to differentiate between different cartilage repair tissues with higher relative $\Delta R1$ values, and thus lower GAG content for cartilage repair tissue after MFX compared to MACT [34]. As the mapping of the GAG concentration is desirable for the diagnosis and monitoring of cartilage pathologies, and the presented dGEMRIC technique has the limitation of contrast agent administration and a time delay before post-contrast MRI, it would be desirable to utilize techniques that do not need any contrast agent. A recently described technique for the assessment of GAG concentration in vivo is chemical exchange-dependent saturation transfer (CEST). Although currently the initial approaches of CEST are done on ultrahigh fields (7.0 Tesla), this technique seems also to be very promising on high (and clinically applicable) fields (3.0 Tesla) [35]. The CEST technique might also be more frequently used in future clinical trials, as, especially for longitudinal evaluation of cartilage repair, the repeated use of i.v. gadolinium is ethically challenging. Furthermore T1rho is seen by different authors as a measure of GAG concentration [36, 37]. Although the specificity to directly quantify proteoglycan content might be less when compared to dGEMRIC and some authors see clear correlations to collagen-sensitive techniques [38], T1rho still is a very promising MR technique to image macromolecules.

## Collagen (Network)-Sensitive Techniques

The most frequently utilized biochemical MR technique is the transverse relaxation time (T2) of cartilage as a sensitive parameter for the evaluation of changes in water and collagen content and tissue anisotropy [39]. So-called cartilage T2 mapping can be obtained relatively easily in a clinical environment with scanning times down to 4 min (3.0 Tesla) and 6 min (1.5 Tesla) for the whole knee joint. Quantitative cartilage T2 mapping reflects the interaction between water and the extracellular matrix on a molecular level. The collagen fiber orientation defines the layers of articular cartilage. Thus, the three-dimensional organization and curvature of the collagen network and the resulting magic angle at 55° (with respect to the main magnetic field (B0)) influence the appearance of T2. In healthy articular cartilage, an increase of these quantitative T2 values can be observed from the subchondral bone up to the cartilage surface. Histologically validated animal studies have shown this zonal increase in T2 values as a marker of hyaline or hyaline-like cartilage structure after cartilage repair procedures within the knee [40, 41]. In cartilage repair tissue, elevated T2 values have been clearly shown in the early postoperative follow-up when compared to the surrounding native cartilage. This T2 elevation adapts over time to T2 values of the surrounding cartilage, which can be seen as a sign of cartilage repair tissue maturation [42]. In other approaches it has been shown that a zonal T2 evaluation is able to assess the quality of the cartilage repair tissue by a differentiation between cartilage repair tissue after MFX and MACT [43]. Whereas cartilage repair tissue after MFX – histologically seen as fibrocartilage – shows no clear zonal increase from deep to superficial cartilage aspects, repair tissue after MACT – histologically reported as hyaline-like – shows a significant stratification.

In addition to standard 2D multi-echo spin-echo sequences used for classic T2 relaxation time mapping, by means of T2*- weighted 3D gradient-echo sequences, additional important biochemical information on cartilage and cartilage repair tissue can be obtained. This so-called T2* mapping has shown reliable results in the evaluation of chondromalacia of the knee [44]. Using this technique, the acquisition time can be reduced down to 2–3 min (3.0 Tesla) for a whole knee joint, and the sequence has the possibility of 3D evaluation. In recent studies, T2* mapping, with these potentially short scan times, was correlated to standard T2 and showed information comparable to that obtained for articular cartilage in the knee, but with overall lower T2* values (ms) [45, 46]. Furthermore, also for T2*, a clear zonal variation between deep and superficial cartilage layers was described for healthy cartilage; after cartilage repair using MFX, however, this stratification could not be found [45]. Thus, for standard T2, as well as for comparable techniques, zonal assessment of healthy and altered articular cartilage is crucial. Nevertheless T2* mapping cannot be interpreted simply as a fast T2 mapping technique, as there are studies that also show a sensitivity for the GAG content of cartilage. Hence T2* mapping should be viewed more as a macromolecule-sensitive technique.

In addition to T2 or T2* mapping, magnetization transfer contrast (MTC) has been shown reliable in the evaluation of the collagen organization and might be more sensitive to the collagen content and less dependent on the hydration of the tissue [47].

## Conclusion

MRI is the gold standard for imaging both in cartilage lesions and cartilage repair sites after therapy. Using high-resolution (if available high-field (3.0 Tesla)) morphological MRI, cartilage and adjacent structures can be depicted in detail. To assess and score the cartilage defect, the AMADEUS score is a promising new tool. For postoperative evaluation of the repair tissue, the MOCART score is a widely accepted instrument. Additionally, it is crucial that the rest of the joint is also visualized in detail to provide information

on other articular comorbidities, e.g., ligament and meniscal injury, or the development of OA. Besides morphological MRI, emerging techniques in biochemical MR imaging are demonstrating very promising results in the evaluation of cartilage physiology and ultrastructure.

## References


1. Recht M, Bobic V, Burstein D, Disler D, Gold G, Gray M, et al. Magnetic resonance imaging of articular cartilage. Clin Orthop Relat Res. 2001 (391 Suppl):S379–96. PubMed PMID: 11603721.
2. Disler DG, McCauley TR, Kelman CG, Fuchs MD, Ratner LM, Wirth CR, et al. Fat-suppressed three-dimensional spoiled gradient-echo MR imaging of hyaline cartilage defects in the knee: comparison with standard MR imaging and arthroscopy. AJR Am J Roentgenol. 1996;167(1):127–32. PubMed PMID: 8659356
3. Peterfy CG, van Dijke CF, Lu Y, Nguyen A, Connick TJ, Kneeland JB, et al. Quantification of the volume of articular cartilage in the metacarpophalangeal joints of the hand: accuracy and precision of three-dimensional MR imaging. AJR Am J Roentgenol. 1995;165(2):371–5. PubMed PMID: 7618560
4. Potter HG, Linklater JM, Allen AA, Hannafin JA, Haas SB. Magnetic resonance imaging of articular cartilage in the knee. An evaluation with use of fast-spin-echo imaging. J Bone Joint Surg Am. 1998;80(9):1276–84. PubMed PMID: 9759811. eng
5. Trattnig S, Huber M, Breitenseher MJ, Trnka HJ, Rand T, Kaider A, et al. Imaging articular cartilage defects with 3D fat-suppressed echo planar imaging: comparison with conventional 3D fat-suppressed gradient echo sequence and correlation with histology. J Comput Assist Tomogr. 1998;22(1):8–14. PubMed PMID: 9448754
6. Kramer J, Recht MP, Imhof H, Stiglbauer R, Engel A. Postcontrast MR arthrography in assessment of cartilage lesions. J Comput Assist Tomogr. 1994;18(2):218–24. PubMed PMID: 7510315. eng
7. Marlovits S, Singer P, Zeller P, Mandl I, Haller J, Trattnig S. Magnetic resonance observation of cartilage repair tissue (MOCART) for the evaluation of autologous chondrocyte transplantation: determination of interobserver variability and correlation to clinical outcome after 2 years. Eur J Radiol. 2006;57(1):16–23. PubMed PMID: 16203119
8. Marlovits S, Striessnig G, Resinger CT, Aldrian SM, Vecsei V, Imhof H, et al. Definition of pertinent parameters for the evaluation of articular cartilage repair tissue with high-resolution magnetic resonance imaging. Eur J Radiol. 2004;52(3):310–9. PubMed PMID: 15544911
9. Jungmann PM, Welsch GH, Brittberg M, Trattnig S, Braun S, Imhoff AB, et al. Magnetic resonance imaging score and classification system (AMADEUS) for assessment of preoperative cartilage defect severity. Cartilage. 2017;8(3):272–82. PubMed PMID: 28618873
10. Azer NM, Winalski CS, Minas T. MR imaging for surgical planning and postoperative assessment in early osteoarthritis. Radiol Clin N Am. 2004;42(1):43–60.
11. Gomoll AH, Yoshioka H, Watanabe A, Dunn JC, Minas T. Preoperative measurement of cartilage defects by MRI underestimates lesion size. Cartilage. 2011;2:389–93.
12. Welsch GH, Zak L, Mamisch TC, Paul D, Lauer L, Mauerer A, et al. Advanced morphological 3D magnetic resonance observation of cartilage repair tissue (MOCART) scoring using a new isotropic 3D proton-density, turbo spin echo sequence with variable flip angle distribution (PD-SPACE) compared to an isotropic 3D steady-state free precession sequence (true-FISP) and standard 2D sequences. J Magn Reson Imaging. 2010;33(1):180–8. PubMed PMID: 21182137. eng
13. Welsch GH, Zak L, Mamisch TC, Resinger C, Marlovits S, Trattnig S. Three-dimensional magnetic resonance observation of cartilage repair tissue (MOCART) score assessed with an isotropic three-dimensional true fast imaging with steady-state precession sequence at 3.0 tesla. Investig Radiol. 2009;44(9):603–12. PubMed PMID: 19692843. eng
14. Apprich S, Mamisch TC, Welsch GH, Stelzeneder D, Albers C, Totzke U, et al. Quantitative T2 mapping of the patella at 3.0T is sensitive to early cartilage degeneration, but also to loading of the knee. Eur J Radiol. 2011.; PubMed PMID: 21497472. Eng
15. Apprich S, Welsch GH, Mamisch TC, Szomolanyi P, Mayerhoefer M, Pinker K, et al. Detection of degenerative cartilage disease: comparison of high-resolution morphological MR and quantitative T2 mapping at 3.0 tesla. Osteoarthr Cartil. 2011;18(9):1211–7. PubMed PMID: 20633680. eng
16. Siebold R, Suezer F, Schmitt B, Trattnig S, Essig M. Good clinical and MRI outcome after arthroscopic autologous chondrocyte implantation for cartilage repair in the knee. Knee Surg Sports Traumatol Arthrosc. 2017.; PubMed PMID: 28258330
17. Mosher TJ, Walker EA, Petscavage-Thomas J, Guermazi A. Osteoarthritis year 2013 in review: imaging. Osteoarthr Cartil. 2013;21(10):1425–35. PubMed PMID: 23891696. eng
18. Roemer FW, Guermazi A, Trattnig S, Apprich S, Marlovits S, Niu J, et al. Whole joint MRI assessment of surgical cartilage repair of the knee: cartilage repair osteoarthritis knee score (CROAKS). Osteoarthr Cartil. 2014;22(6):779–99. PubMed PMID: 24685525
19. Eshed I, Trattnig S, Sharon M, Arbel R, Nierenberg G, Konen E, et al. Assessment of cartilage repair after chondrocyte transplantation with a fibrin-hyaluronan matrix--correlation of morphological MRI, biochemi-

cal T2 mapping and clinical outcome. Eur J Radiol. 2012;81(6):1216–23. PubMed PMID: 21458942
20. Peterfy CG, Guermazi A, Zaim S, Tirman PF, Miaux Y, White D, et al. Whole-organ magnetic resonance imaging score (WORMS) of the knee in osteoarthritis. Osteoarthr Cartil. 2004;12(3):177–90. PubMed PMID: 14972335
21. Kornaat PR, Ceulemans RY, Kroon HM, Riyazi N, Kloppenburg M, Carter WO, et al. MRI assessment of knee osteoarthritis: knee osteoarthritis scoring system (KOSS)--inter-observer and intra-observer reproducibility of a compartment-based scoring system. Skelet Radiol. 2005;34(2):95–102. PubMed PMID: 15480649
22. Hunter DJ, Guermazi A, Lo GH, Grainger AJ, Conaghan PG, Boudreau RM, et al. Evolution of semi-quantitative whole joint assessment of knee OA: MOAKS (MRI osteoarthritis knee score). Osteoarthr Cartil. 2011;19:990–1002.
23. Soellner ST, Goldmann A, Muelheims D, Welsch GH, Pachowsky ML. Intraoperative validation of quantitative T2 mapping in patients with articular cartilage lesions of the knee. Osteoarthr Cartil. 2017.; PubMed PMID: 28801212
24. Zbyn S, Mlynarik V, Juras V, Szomolanyi P, Trattnig S. Evaluation of cartilage repair and osteoarthritis with sodium MRI. NMR Biomed. 2016;29(2):206–15. PubMed PMID: 25810325
25. Kretzschmar M, Bieri O, Miska M, Wiewiorski M, Hainc N, Valderrabano V, et al. Characterization of the collagen component of cartilage repair tissue of the talus with quantitative MRI: comparison of T2 relaxation time measurements with a diffusion-weighted double-echo steady-state sequence (dwDESS). Eur Radiol 2015;25(4):980–6. PubMed PMID: 25407662.
26. Jungmann PM, Baum T, Bauer JS, Karampinos DC, Erdle B, Link TM, et al. Cartilage repair surgery: outcome evaluation by using noninvasive cartilage biomarkers based on quantitative MRI techniques? Biomed Res Int. 2014;2014:840170. PubMed PMID: 24877139. Pubmed Central PMCID: 4024422
27. Bekkers JE, Bartels LW, Vincken KL, Dhert WJ, Creemers LB, Saris DB. Articular cartilage evaluation after TruFit plug implantation analyzed by delayed gadolinium-enhanced MRI of cartilage (dGEMRIC). Am J Sports Med. 2013.; PubMed PMID: 23585485. Eng
28. Schmitt B, Zbyn S, Stelzeneder D, Jellus V, Paul D, Lauer L, et al. Cartilage quality assessment by using glycosaminoglycan chemical exchange saturation transfer and (23)Na MR imaging at 7 T. Radiology. 2012;260(1):257–64. PubMed PMID: 21460030. eng
29. Bashir A, Gray ML, Boutin RD, Burstein D. Glycosaminoglycan in articular cartilage: in vivo assessment with delayed Gd(DTPA)(2-)-enhanced MR imaging. Radiology. 1997;205(2):551–8. PubMed PMID: ISI:A1997YD15100042
30. Tiderius CJ, Olsson LE, Leander P, Ekberg O, Dahlberg L. Delayed gadolinium-enhanced MRI of cartilage (dGEMRIC) in early knee osteoarthritis. Magnet Reson Med. 2003;49(3):488–92. PubMed PMID: ISI:000181297200011
31. Williams A, Gillis A, McKenzie C, Po B, Sharma L, Micheli L, et al. Glycosaminoglycan distribution in cartilage as determined by delayed gadolinium-enhanced MRI of cartilage (dGEMRIC): potential clinical applications. Am J Roentgenol. 2004;182(1):167–72. PubMed PMID: ISI:000188495900040
32. Watanabe A, Wada Y, Obata T, Ueda T, Tamura M, Ikehira H, et al. Delayed gadolinium-enhanced MR to determine glycosaminoglycan concentration in reparative cartilage after autologous chondrocyte implantation: preliminary results. Radiology. 2006;239(1):201–8. PubMed PMID: ISI:000236669100026
33. Trattnig S, Burstein D, Pinker K, Szomolanyi P, Welsch GH, Mamisch TC. T1(Gd) gives comparable information as delta T1 relaxation rate in dGEMRIC evaluation of cartilage repair tissue. Investig Radiol. 2009:In Press.
34. Trattnig S, Mamisch TC, Pinker K, Domayer S, Szomolanyi P, Marlovits S, et al. Differentiating normal hyaline cartilage from post-surgical repair tissue using fast gradient echo imaging in delayed gadolinium-enhanced MRI (dGEMRIC) at 3 tesla. Eur Radiol. 2008.; PubMed PMID: 18246356. Eng
35. Ling W, Regatte RR, Navon G, Jerschow A. Assessment of glycosaminoglycan concentration in vivo by chemical exchange-dependent saturation transfer (gagCEST). Proc Natl Acad Sci U S A. 2008;105(7):2266–70. PubMed PMID: 18268341. eng
36. Regatte RR, Akella SV, Lonner JH, Kneeland JB, Reddy R. T1rho relaxation mapping in human osteoarthritis (OA) cartilage: comparison of T1rho with T2. J Magn Reson Imaging. 2006;23(4):547–53. PubMed PMID: 16523468
37. Borthakur A, Mellon E, Niyogi S, Witschey W, Kneeland JB, Reddy R. Sodium and T1rho MRI for molecular and diagnostic imaging of articular cartilage. NMR Biomed. 2006;19(7):781–821. PubMed PMID: 17075961. Epub 2006/11/01. eng
38. Mlynarik V, Szomolanyi P, Toffanin R, Vittur F, Trattnig S. Transverse relaxation mechanisms in articular cartilage. J Magn Reson. 2004;169(2):300–7. PubMed PMID: 15261626
39. Mosher TJ, Dardzinski BJ, Cartilage MRI. T2 relaxation time mapping: overview and applications. Semin Musculoskelet Radiol. 2004;8(4):355–68. PubMed PMID: 15643574
40. Watrin-Pinzano A, Ruaud JP, Cheli Y, Gonord P, Grossin L, Bettembourg-Brault I, et al. Evaluation of cartilage repair tissue after biomaterial implantation in rat patella by using T2 mapping. Magn Reson Mater Phy. 2004;17(3–6):219–28. PubMed PMID: 15580373

41. White LM, Sussman MS, Hurtig M, Probyn L, Tomlinson G, Kandel R. Cartilage T2 assessment: differentiation of normal hyaline cartilage and reparative tissue after arthroscopic cartilage repair in equine subjects. Radiology 2006;241(2):407–14. PubMed PMID: 17057068.
42. Trattnig S, Mamisch TC, Welsch GH, Glaser C, Szomolanyi P, Gebetsroither S, et al. Quantitative T2 mapping of matrix-associated autologous chondrocyte transplantation at 3 tesla: an in vivo cross-sectional study. Investig Radiol. 2007;42(6):442–8. PubMed PMID: 17507817. eng
43. Welsch GH, Mamisch TC, Domayer SE, Dorotka R, Kutscha-Lissberg F, Marlovits S, et al. Cartilage T2 assessment at 3-T MR imaging: in vivo differentiation of normal hyaline cartilage from reparative tissue after two cartilage repair procedures--initial experience. Radiology. 2008;247(1):154–61. PubMed PMID: 18372466. eng
44. Murphy BJ. Evaluation of grades 3 and 4 chondromalacia of the knee using T2*-weighted 3D gradient-echo articular cartilage imaging. Skelet Radiol 2001;30(6):305–11. PubMed PMID: 11465769.
45. Hughes T, Welsch GH, Trattnig S, Brandi L, Domayer S, Mamisch TC. T2-star relaxation as a means to Diffrentiatie cartilage repair tissue after microfracturing therapy. Intern Soc. Magn Reson Med. 2007;15:183.
46. Wietek B, Martirosian P, Machann J, Mueller-Horvath C, Claussen CD, Schick F. T2 and T2* mapping of the human femoral-Tibial cartilage at 1.5 and 3 tesla. Intern Soc. Magn Reson Med. 2007;15:516.
47. Welsch GH, Trattnig S, Scheffler K, Szomonanyi P, Quirbach S, Marlovits S, et al. Magnetization transfer contrast and T2 mapping in the evaluation of cartilage repair tissue with 3T MRI. J Magn Reson Imaging. 2008;28(4):979–86. PubMed PMID: 18821633. Epub 2008/09/30. eng